Journal of
Mechanical
Science and
Technology

Journal of Mechanical Science and Technology 21 (2007) 1388~1397

# On the Aerodynamic Forces of a Plunging Airfoil

John Young, Joseph C. S. Lai*

*School of Aerospace, Civil & Mechanical Engineering,*
*University of New South Wales, Australian Defence Force Academy,*
*Northcott Drive, Canberra ACT 2600, Australia.*

(Manuscript Received November 23, 2006; Revised March 23, 2007; Accepted May 2, 2007)

**Abstract**

The generation of aerodynamic forces by a plunging NACA0012 airfoil at a Reynolds number of 20,000 was studied for a range of non-dimensional plunge frequencies $k$ and amplitudes $h$ using a 2D unsteady compressible Navier-Stokes solver, an unsteady panel method (UPM) and Garrick's analysis. Calculations using these two methods indicate that the forces collapse reasonably well with $kh$ (or equivalently the Strouhal number), but are only weak functions of $k$. In contrast results from the NS code indicate that the forces are dependent on both $k$ and $kh$ independently, with large variations at low frequencies. The frequency dependence was found to be a result of vortex shedding from the leading edge of the airfoil, and appears to result from two factors. Firstly at high plunge frequencies $k$, the leading edge vortex does not have sufficient time to grow, whereas at low $k$ the vortex can become a sizeable fraction of the airfoil chord before separating. Secondly once the vortex separates, it is convected downstream over the surface of the airfoil. Due to the low pressure in the vortex core, thrust is maintained while the vortex is upstream of the airfoil maximum thickness point (where the airfoil surface is tilted upstream and the vortex low pressure creates an upstream suction force). Once past this point, the airfoil surface is tilted downstream and the vortex contributes to drag rather than thrust. At high plunge frequencies the vortex cannot be convected far downstream before the motion cycle creates another leading edge vortex on the opposite side of the airfoil, so the impact is lessened. At low $k$ however the vortex travels far downstream over the airfoil surface, causing drag for a larger portion of the flapping cycle, and therefore lower propulsive efficiency. These results have strong implications on how the thrust and the propulsive efficiency can be maximised by controlling the relative amplitudes and phases of combined pitching and plunging motions of an airfoil.

*Keywords*: Plunging airfoil; Oscillating airfoil; Thrust generation; Navier-Stokes solver; Unsteady panel method

## 1. Introduction

Oscillating airfoils have been attracting increased attention because of their importance in understanding the physics involved in many practical applications such as the dynamic stall phenomenon (Choudhuri et al., 1994; Ekaterinaris and Platzer, 1997; Isogai et al., 1999), propulsion of fish and marine animals(Lighthill, 1960; Traintafyllou et al., 1993; Bandyopadhyay et al., 2000), and the use of flapping wings in generating lift and propulsion in micro air vehicles (Shyy et al., 1999). There have been many studies demonstrating thrust generation by a oscillating an airfoil in purely pitching motion (Koochesfahani, 1989), purely plunging motion (Lai and Platzer, 1999) or a combination of pitching and plunging motion (Anderson, 1998). Nevertheless, the mechanism for thrust generation is not fully understood. The objective of this paper is, therefore, to present results of a study focussed on the generation of aerodynamic forces by a NACA0012 airfoil undergoing purely plunging motion at a Reynolds

*Corresponding author. Tel.: +61 2 6268 8272, Fax.: +61 2 6268 8276
E-mail address: j.lai@adfa.edu.au

number of 20,000 for a range of non-dimensional plunge frequencies $k$ and $h$, using a 2D unsteady compressible Navier-Stokes solver, an unsteady panel method (UPM) and Garrick's linear analysis (1937).

## 2. Analytical and numerical methods

### 2.1 Garrick's linearized potential analysis

For a plunging flat plate, the time-averaged thrust coefficient per unit span $C_{Tmean}$, and the single-sided peak lift coefficient per unit span $C_{Lpeak}$, were determined respectively by Garrick (1937) as a function of the non-dimensional plunge amplitude $h$ and reduced frequency $k$:

$$C_{Tmean}=4\pi(kh)^2 A \quad C_{Lpeak}=4\pi(kh)B \tag{1}$$

where $A=\left(F^2+G^2\right)$; $B=\left(F^2+G^2+kG+k^2/4\right)^{1/2}$;

$F = F(k)$ and $G = G(k)$ are the real and imaginary components of the Theodorsen Function $C(k) = F(k) + i\,G(k)$. The $A$ term asymptotes to a constant value 0.25 for large $k$ (approximately $k > 4.0$), so that $C_{Tmean}$ depends only on the single parameter $kh$ for large enough $k$.

### 2.2 Two-dimensional compressible Navier-Stokes solver

The unsteady flow field around an airfoil undergoing a purely sinusoidal plunging motion was simulated using a 2nd order accurate 2D compressible Navier Stokes (NS) solver, at low Mach number ($M_\infty$ = 0.05 or 0.025). The equations were solved on a structured C-grid wrapped around the airfoil, using Crank-Nicolson 2nd-order time discretization with viscous flux terms evaluated by 2nd-order central differences in space, and inviscid fluxes by a 3rd-order accurate Osher upwind scheme. The resulting semi-implicit equations were solved using Newton sub-iterations. The motion of the airfoil was introduced by a combination of rigid-body motion and deformation of the grid. Details of the method and quantitative and qualitative validation against results in the literature were reported by Young and Lai (2004). Results presented here use a 541 × 61 grid (377 points around the airfoil surface, first normal grid point at $9.2\times10^{-5}$ chord-lengths from the surface), boundaries at 20 chords from the airfoil, and non-dimensional time-step $\Delta t = 4.7\times10^{-4}$ for which the aerodynamic forces are grid and time-step independent.

### 2.3 Unsteady panel method

In the analysis of Garrick (1937), small amplitudes of motion of a flat plate were assumed and vorticity was shed in the form of a continuous vortex sheet on the centreline of motion but the evolution of the vortex sheet in response to self-induced velocities was not allowed. Thus an unsteady panel method (UPM) code was developed following Basu and Hancock (1978) and Jones et al. (1996). The method allows arbitrary airfoil shapes, assumes inviscid and incompressible flow, enforces the Kutta condition at the trailing edge, and does not allow any separation over the airfoil surface. As the airfoil translates and the lift changes, vorticity is shed into the wake at each time step as a series of discrete point vortices which are convected due to free-stream and self-induced velocities, thus the non-linear character of the wake is preserved. Results presented here used 400 panels around the airfoil, and 200 Rankine vortices shed into the wake per plunge cycle. The UPM code cannot simulate viscous effects or leading-edge shedding of vorticity, so comparison with Navier-Stokes (NS) results will determine the importance of viscous and separation effects.

## 3. Comparison of aerodynamic force calculations with experiments

The NS code was validated by Young and Lai (2004) using the flow visualization results of Lai and Platzer (1999). The mean thrust coefficient $C_{Tmean}$ of a plunging airfoil at $Re$ = 1,100 – 2,200 for a range of $k$ and $h$ was estimated by Lai and Platzer (1999) from the spatially averaged momentum fluxes determined using LDV measured mean streamwise velocity profiles from $x/c$ = 1.8 – 15. Figure 1 shows the comparison of $C_{Tmean}$ determined from momentum fluxes by Lai and Platzer (1999) and that determined from the NS solver for various integration limits in the transverse direction ($y/c$). There is a reasonably good agreement between the NS and Lai and Platzer (1999) results. Furthermore, $C_{Tmean}$ determined from NS pressure and viscous force (surface) results are well below the Garrick values, suggesting that the NS code is capturing a parameter dependence not accounted for in the Garrick analysis.

The results obtained from Garrick, UPM and NS methods for $C_{Lpeak}$, $C_{Tmean}$ and $C_{Mpeak}$ as a function of $k$

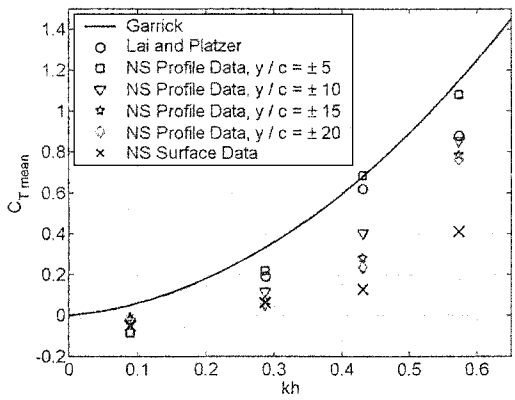


Fig. 1. Comparison of $C_{Tmean}$ determined from momentum fluxes obtained by LDV and NS solutions, and $C_{Tmean}$ determined from NS pressure and viscous force (surface) data.

at $kh = 0.3$ are shown in Figs. 2(a),(b) and (c) respectively. It is clear that results from both the Garrick and UPM methods follow each other very closely and that $C_{Tmean}$ is essentially constant for $k > 4$, as expected from the analysis Sec. 2.1.1. On the other hand, although the trend predicted by the NS solver for the variation of $C_{Lpeak}$ and $C_{Mpeak}$ with $k$ is very similar to the Garrick and UPM results, it is very different for $C_{Tmean}$. While all three methods predict that $C_{Tmean}$ is virtually independent of $k$ for $k > 4$, the NS results indicate a sharp drop in thrust $C_{Tmean}$ as $k$ is reduced, contrary to the prediction of Garrick and UPM that there is a sharp increase in thrust with decreasing $k$. This difference in the thrust behaviour will be examined in detail in Sec. 4.

Figure 3 displays the comparisons of mean thrust coefficient $C_{Tmean}$, mean power coefficient $C_{Pmean}$ and propulsive efficiency η obtained from Garrick's analysis, UPM and NS solver with measurements made by Heathcote et al. (2006) for a NACA0012 airfoil undergoing a pure plunging motion with amplitude $h = 0.175$, reduced frequency in the range $k = 0$ to 6.3, and Reynolds number $Re = 10{,}000$, 20,000 and 30,000. NS calculations were made for laminar flow at $Re = 20{,}000$. It can be seen that the NS solver reproduces the experimentally measured mean thrust and power coefficients very well at all values of $kh$. Although the experimentally measured propulsive efficiency is slightly over-predicted by the NS solver at intermediate $kh = 0.2$-$0.6$, its trend is well predicted with a peak close to the correct magnitude and $kh$ and very similar rapid drop-off at low $kh$ and gradual drop-off at high $kh$. On the other hand, both the

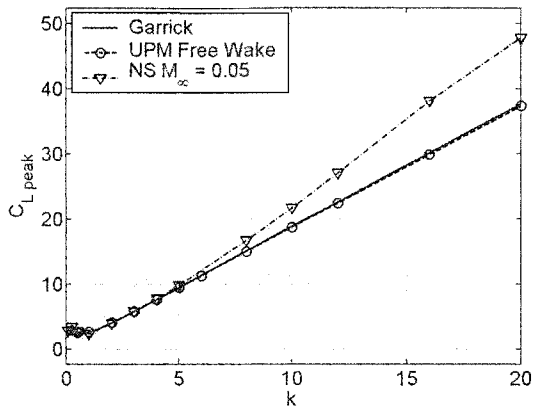


Fig. 2(a). Comparison of $C_{Lpeak}$ determined from Garrick, UPM and NS ($M_\infty$=0.05, laminar) results,

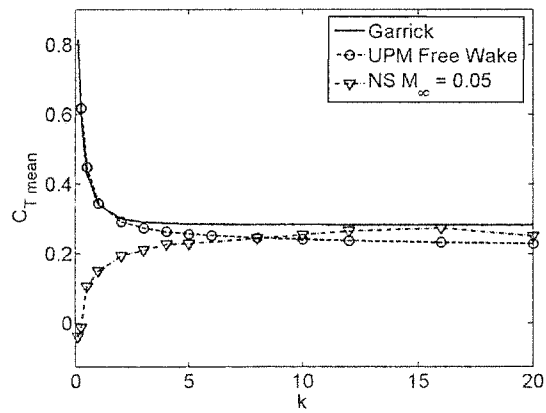


Fig. 2(b). Comparison of $C_{Tmean}$ determined from Garrick, UPM and NS (M=0.05, laminar) results, $kh = 0.3$.

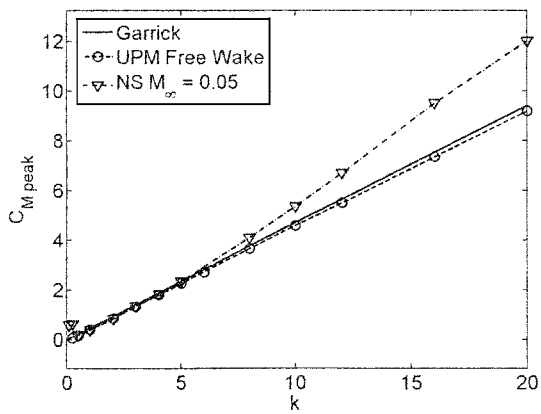


Fig. 2(c). Comparison of $C_M$ determined from Garrick, UPM and NS ($M_\infty$=0.05, laminar) results, $kh = 0.3$.

Garrick and UPM methods over-predict the thrust and under-predict the input power, resulting in much higher propulsive efficiencies. Furthermore, both the

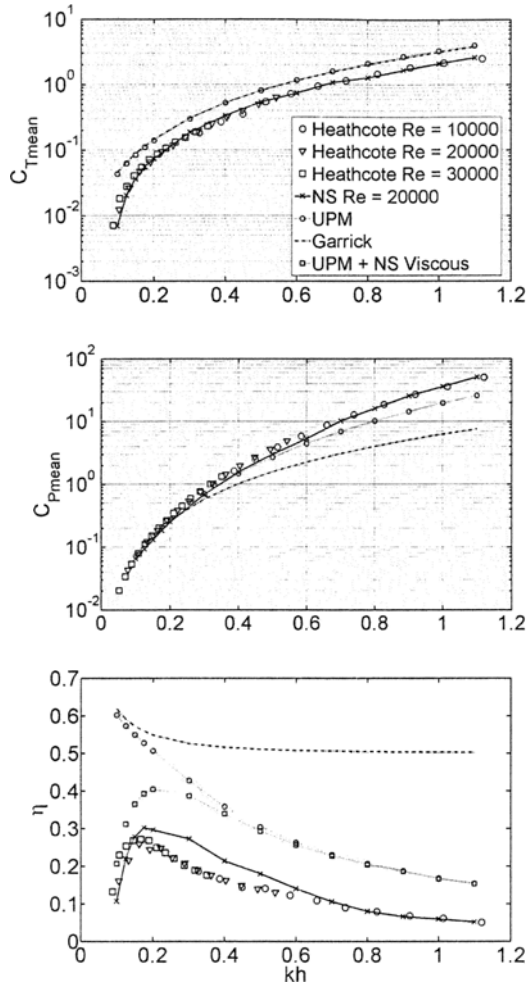


Fig. 3. Comparison of experimental (Heathecote et al., 2006), Navier-Stokes (NS) laminar, UPM and Garrick's results for mean thrust coefficient, mean power coefficient and propulsive efficiency. Pure plunging motion ($h = 0.175$).

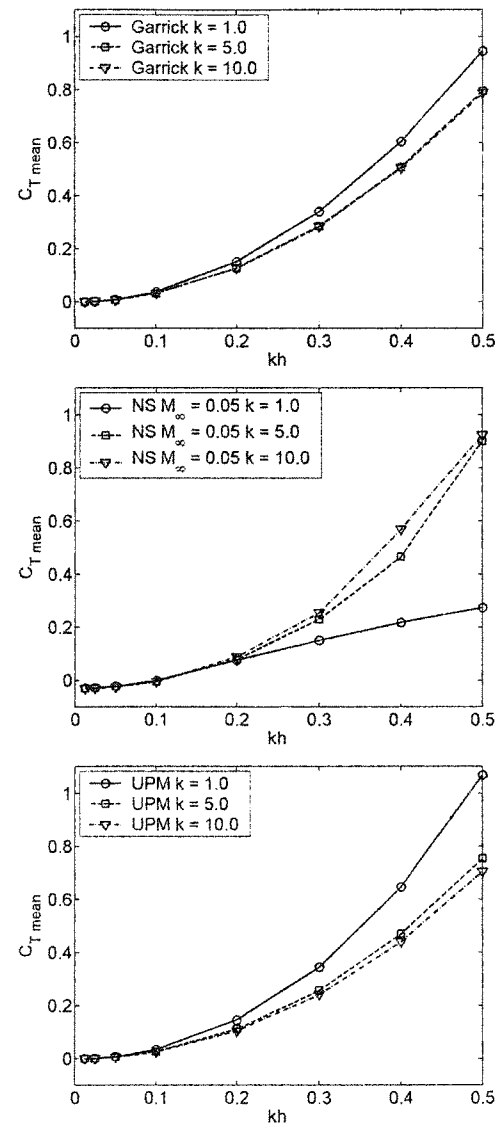


Fig. 4. Comparison of the variation of $C_{Tmean}$ with $kh$ predicted by Garrick, UPM and NS (laminar).

Garrick and UPM results fail to predict the peak in $\eta$ as observed experimentally. This failure is partially due to the lack of viscous drag in these inviscid methods. When the stationary airfoil drag predicted by the NS code is added to the UPM results, a peak is now predicted at approximately the correct $kh$ but the magnitude is still too high. It is worth noting that the thrust results based on the Garrick and UPM methods are virtually identical, indicating that the non-linear roll-up of the wake (allowed in UPM but not by Garrick) has little effect on the thrust generated, in agreement with the findings of Hall and Hall (2000).

The effect of $k$ and $kh$ on the generated thrust $C_{Tmean}$ as predicted by the Garrick, UPM and NS methods is summarised in Fig. 4. While the results from all three methods indicate that $C_{Tmean}$ is a strong function of $kh$, both the Garrick and UPM methods predict that $C_{Tmean}$ is a weak function of $k$ with slight increases at low $k$. The increase in $C_{Tmean}$ with decreasing $k$ at low $k$ for a given $kh$, as predicted by the Garrick and UPM methods may be attributed to the increase in the strength of vortices shed at the trailing edge. On the other hand, the NS results in agreement with measurements indicate a substantial loss in $C_{Tmean}$ at low $k$, suggesting that the thrust generation is influenced by mechanisms in addition to the

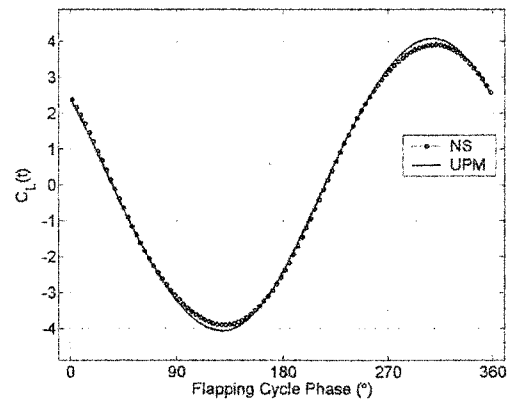


Fig. 5(a). Instantaneous lift coefficient due to pressure forces only. NS ($M_\infty$=0.025 laminar) and UPM comparison, $k$ = 2.0, $h$ = 0.15.

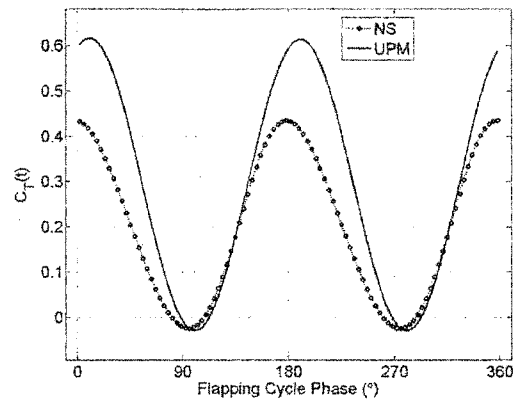


Fig. 5(c). Instantaneous thrust coefficient due to pressure forces only. NS ($M_\infty$=0.025 laminar) and UPM comparison, $k$ = 2.0, $h$ = 0.15.

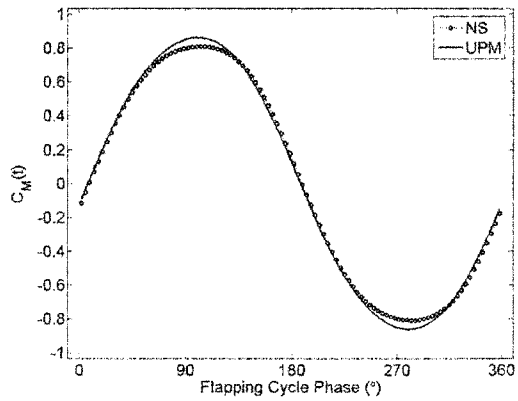


Fig. 5(b). Instantaneous moment coefficients due to pressure forces only. NS ($M_\infty$=0.025 laminar) and UPM comparison, $k$ = 2.0, $h$ = 0.15.

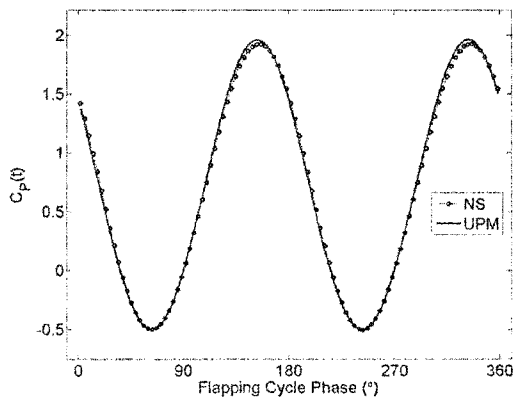


Fig. 5(d). Instantaneous input power coefficient due to pressure forces only. NS ($M_\infty$ =0.025 laminar) and UPM comparison, $k$ = 2.0, $h$ = 0.15.

dynamics of vortices shed at the trailing edge.

## 4. The role of leading edge vortex shedding

In order to understand the differences between inviscid analysis (Garrick and UPM) and viscous analysis (NS) in the predicted behaviour of the generated thrust at low $k$, the time histories of the lift, moment (positive about the quarter-chord), thrust and input power coefficients (determined from pressure distributions around the airfoil predicted by UPM and NS and ignoring viscous forces) for one plunge cycle, $kh$ = 0.3 and $k$ = 2 are shown in Fig. 5. The NS calculations were made for laminar flow with $M_\infty$ = 0.025 and $Re$ = 20,000. It can be seen from Fig. 5 that while there is good agreement between the UPM and NS results for lift, moment and input power, the thrust predicted by the NS solver is significantly less than that predicted by the UPM. This difference in the predicted thrust $C_{Tmean}$ could be more readily explained by examining the surface pressure coefficient distributions in Fig. 6 for four phases of the plunge cycle: $\phi$ = 0°, 45°, 90° and 135°. Here $\phi$ = 0° refers to the airfoil at the centreline moving downwards. There is very good agreement between UPM and NS results for the airfoil surface pressure coefficient distributions, except close to the leading edge. Figure 6 clearly shows that the NS simulation predicts the formation of a leading edge vortex and consequently the pressure coefficient is not as low as the spike predicted by the UPM near the leading edge. This leading edge vortex is seen to convect downstream over the airfoil and to diffuse. As long

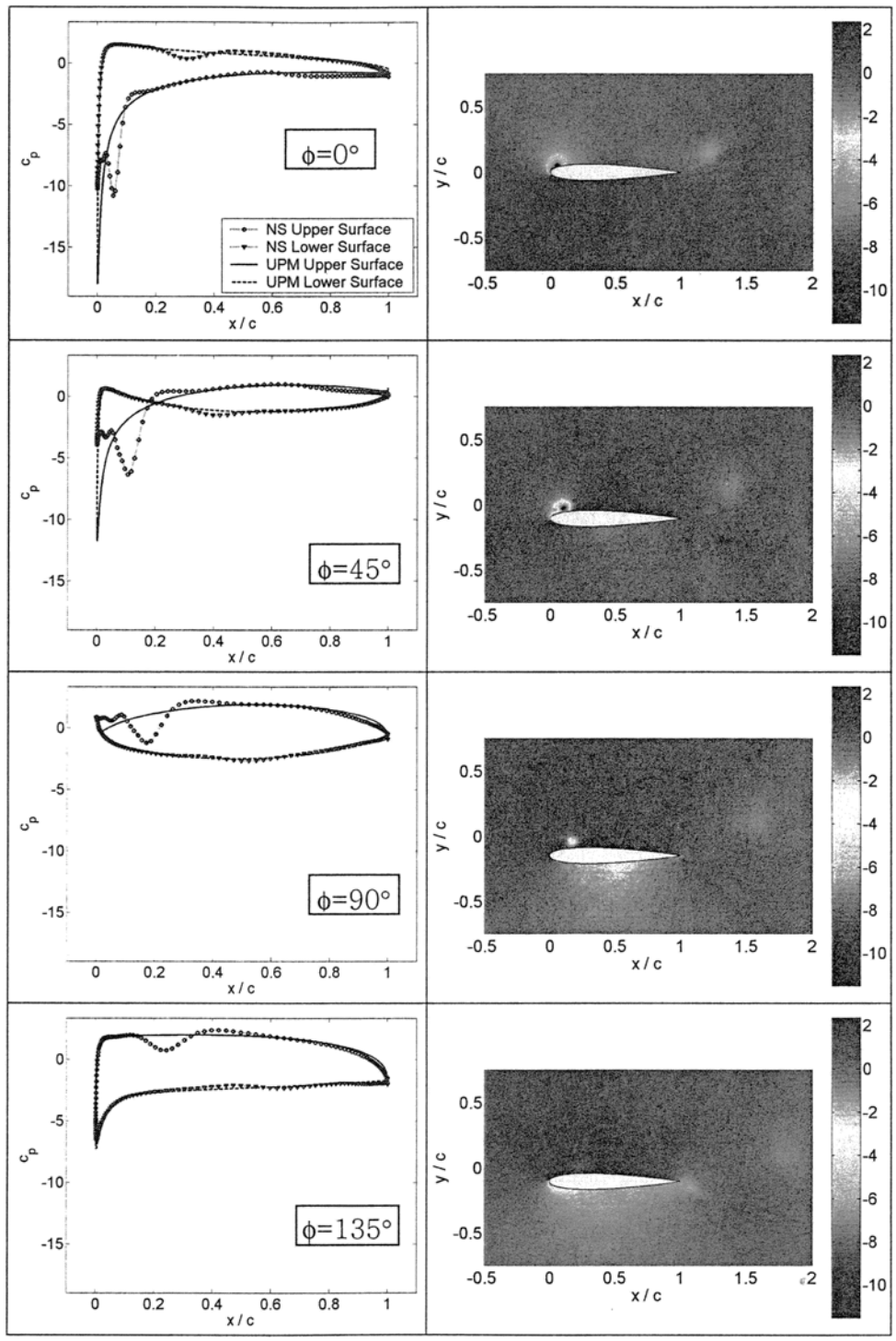


Fig. 6. Pressure coefficient, NS ($M_\infty$=0.025 laminar) and UPM surface comparison (left), and NS field results (right), $k = 2.0$, $h = 0.15$.

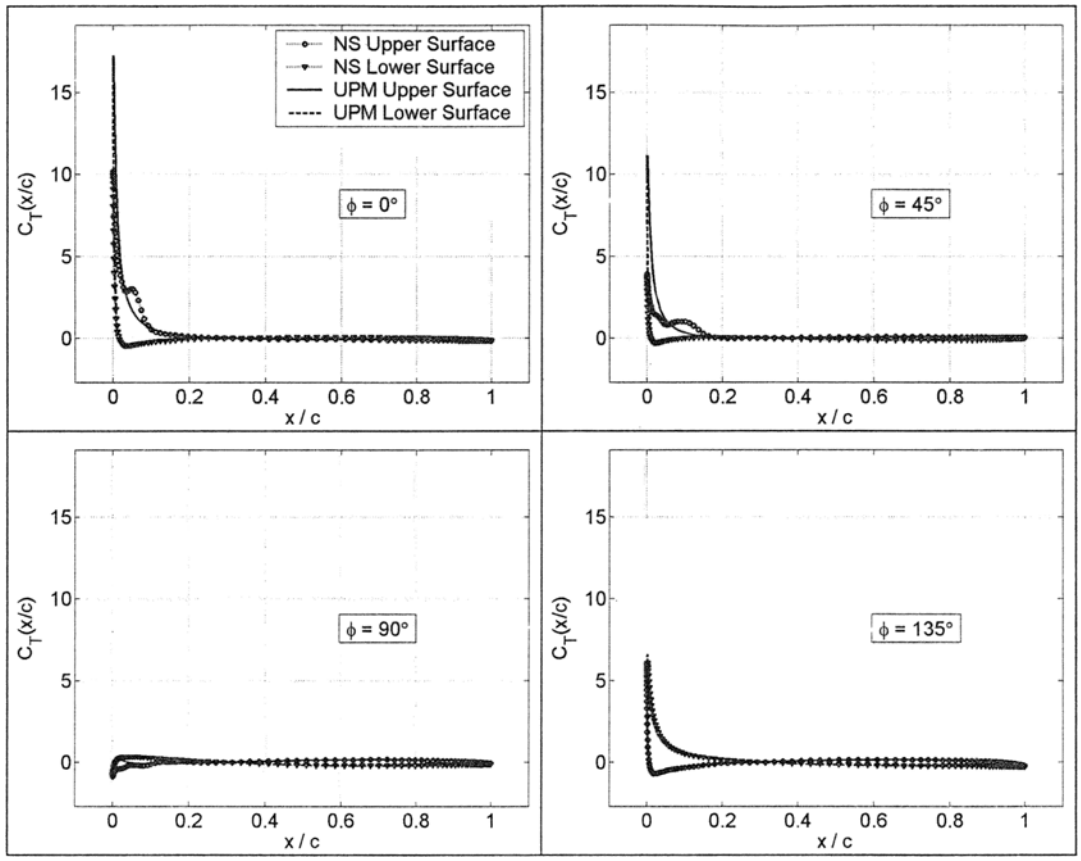


Fig. 7. Chordwise distributions of pressure-induced thrust for $k = 2$, $h = 0.15$.

as the vortex remains upstream of the point of airfoil maximum thickness, it contributes towards thrust but as it travels aft of this point, its contributes to drag, with very little effect on the lift generation, as already seen in Fig. 5. As shown in Fig. 7, the corresponding chordwise distributions of the thrust coefficient $C_T$ developed along the airfoil surface at each phase, due solely to the pressure, clearly indicate that the reduction in thrust predicted by the NS solver is due to the leading edge vortex.

In order to examine the effect of the leading edge vortex at high $k$, the surface pressure coefficient distributions for $kh = 0.3$ and $k = 8$ are shown in Fig. 8 for four phases of the plunge cycle $\phi = 0°$, 45° ,90° and 135°. It can be seen that the size of the leading edge vortex is much smaller and consequently its effect on the airfoil surface pressure distribution is much reduced. Hence, as shown in Fig. 2(b), the thrust $C_{Tmean}$ predicted by both the UPM and NS methods is in good agreement. The frequency dependence of the generated thrust on $k$ for a given $kh$ can be explained as follows. As $k$ increases, the period of the airfoil motion decreases. On the other hand, the rate at which the flow can respond to a developing low pressure suction peak, by separating and forming a leading edge vortex, is fixed by the oncoming flow conditions, resulting in a relatively constant convection speed of the vortex. Consequently, there is less time for the vortex to form and less time to travel downstream along the airfoil past the point of maximum thickness, where it contributes drag instead of thrust and reduces the propulsive efficiency. Furthermore, the leading edge vortex has a smaller relative effect on the airfoil surface pressure distribution at higher $k$, because as evident from Figs. 6 and 8, the pressure extremes developed around the airfoil during the plunging cycle are greater with increasing $k$. Thus the frequency dependence of the thrust predicted by the NS solver in Fig. 4 may be manipulated to yield an optimal plunging frequency

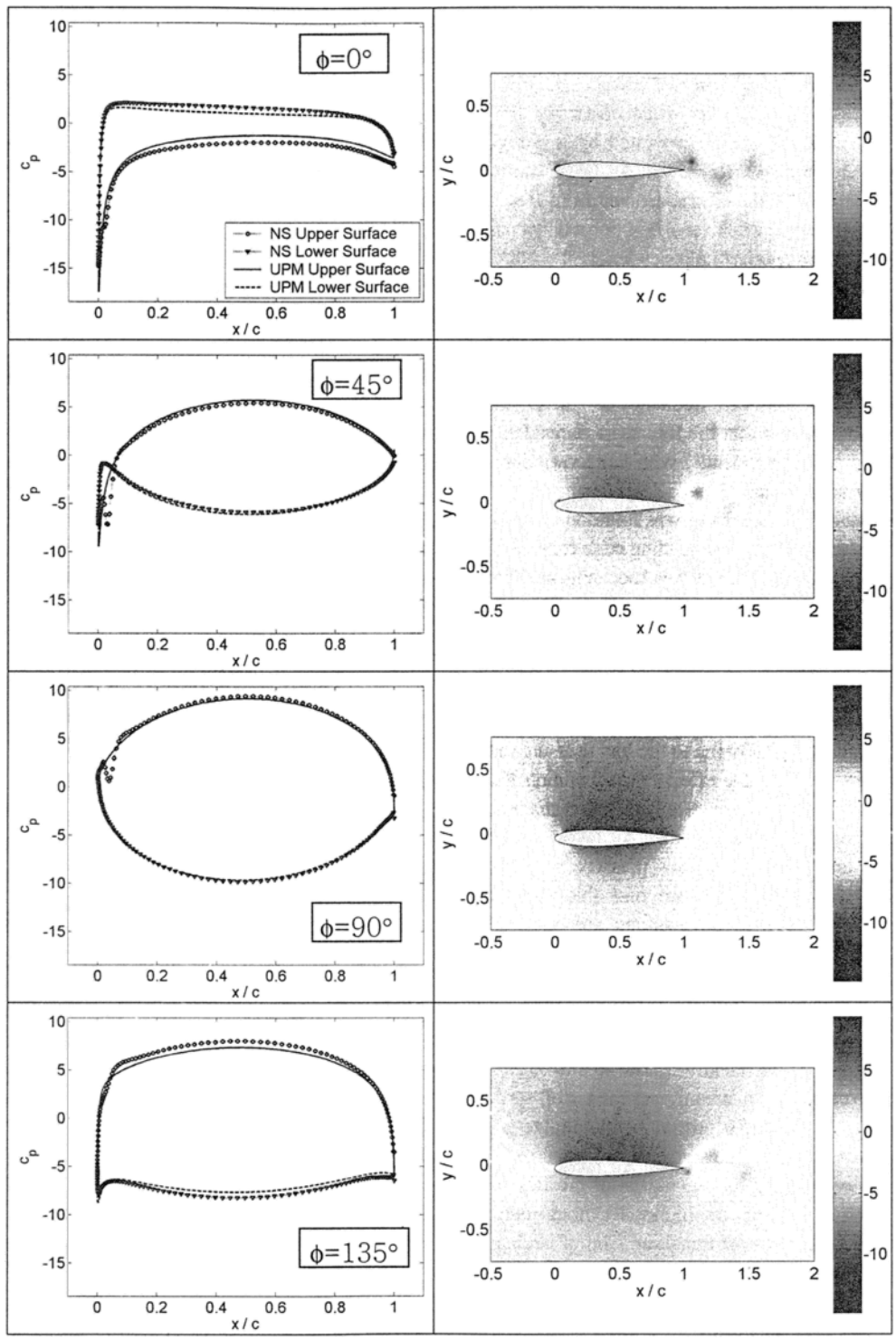


Fig. 8. Pressure coefficient, NS ($M_\infty$=0.025 laminar) and UPM surface comparison (left), and NS field results (right), $k$ = 8.0, $h$ = 0.0375.

for maximum propulsive efficiency.

## 5. Conclusion

The aerodynamic forces generated by a plunging NACA0012 airfoil at Re = 20,000 were examined across a range of reduced frequencies from $0 < k < 20.0$, using the Garrick analysis, unsteady panel method code and Navier-Stokes code.

The Garrick analysis and UPM code, which apply the Kutta condition and do not allow for flow separation, predict that the forces increase with $kh$ (or equivalently the Strouhal number) but are only weak functions of the reduced frequency $k$. In contrast, the NS code showed that the forces are dependent on both $k$ and $kh$ independently, with large variations at low frequencies.

The frequency dependence was found to be a result of vortex shedding from the leading edge of the airfoil, and it appears to result from two mechanisms. Firstly at high plunge frequencies $k$, the leading edge vortex does not have sufficient time to grow, whereas at low $k$ the vortex can become a sizeable fraction of the airfoil chord before separating. Secondly once the vortex separates, it is convected downstream over the surface of the airfoil. Owing to the low pressure in the vortex core, this has the effect of maintaining thrust while the vortex is upstream of the airfoil maximum thickness point (where the airfoil surface is tilted upstream and the vortex low pressure creates an upstream suction force). Once past this point, the airfoil surface is tilted downstream and the vortex contributes to drag rather than thrust. At high plunge frequencies, the vortex cannot be convected far downstream before the motion cycle creates another leading edge vortex on the opposite side of the airfoil, so the impact is lessened. At low $k$ ,however, the vortex travels far downstream over the airfoil surface, causing drag for a larger portion of the plunge cycle, and therefore lower propulsive efficiency.

Clearly controlling the separation of the flow near the leading edge, and for higher Reynolds number flows, the exact point of transition from a laminar to turbulent boundary layer, will play a crucial role in determining the thrust development of the airfoil. This effect of the leading edge vortex can be manipulated by combined pitching and plunging motions (Schouveiler et al., 2005), where the orientation of the airfoil surface is controlled by the relative amplitudes and phases of such motion so that the vortex may create positive thrust for much longer portions of the flapping cycle and thus contribute towards the propulsive efficiency rather than detract from it.

## Nomenclautre

$a$ : Single-sided plunge amplitude
$a_\infty$ : Free stream speed of sound
$c$ : Airfoil chord
$c_p$ : Pressure coefficient
$C_{Lpeak}$ : Single-sided-peak lift coefficient per unit span
$C_{Tmean}$ : Time-averaged thrust coefficient per unit span
$C_{Pmean}$ : Time-averaged power coefficient per unit span
$f$ : Plunge frequency in Hz
$h$ : Non-dimensional plunge amplitude $a/c$
$k$ : Reduced frequency $\omega c/(2U_\infty)$
$M_\infty$ : Free stream Mach number
$Re$ : Reynolds number based on airfoil chord
$T$ : Non-dimensional plunge period $2\pi a_\infty/(\omega c) = \pi/(kM_\infty)$
$U_\infty$ : Free stream velocity
$\eta$ : Propulsive efficiency
$\omega$ : Angular frequency $2\pi f$

## References

Anderson, J. M., Streitlien, K., Barrett, D. S. and Triantafyllou, M. S., 1998, "Oscillating Foils Of High Propulsive Efficiency," *Journal of Fluid Mechanics*, Vol. 360, pp. 41~72.

Bandyopadhyay, P. R., Castano, J. M., Nedderman, W. H. and Donnelly, M. J., 2000, "Experimental Simulation of Fish-Inspired Unsteady Vortex Dynamics on a Rigid Cylinder," *ASME Journal of Fluids Engineering*, Vol. 122( 2), pp. 219~238.

Basu, B. C. and Hancock, G. J., 1978, "The Unsteady Motion of a Two-Dimensional Aerofoil in Incompressible Inviscid Flow," *Journal of Fluid Mechanics*, Vol. 87(1), pp. 159~178.

Choudhuri, P. G., Knight, D. D. and Visbal, M. R., 1994, "Two-Dimensional Unsteady Leading-Edge Separation on a Pitching Airfoil," *AIAA Journal*, Vol. 32(4), pp. 673~680.

Ekaterinaris, J. A. and Platzer, M. F., 1997,

"Computational Prediction of Airfoil Dynamic Stall," in *Progress in Aerospace Sciences*, Vol. 33, pp. 759~846.

Garrick, I. E., 1937, "Propulsion of a Flapping and Oscillating Airfoil," *NACA Report* 567.

Hall, K. C. and Hall, S. R., 2000, "A Rational Engineering Analysis Of The Efficiency Of Flapping Flight," *in Fixed and flapping wing aerodynamics for micro air vehicle applications,* edited by T.J. Mueller, AIAA, Reston, VA, pp. 249~274.

Heathcote, S., Wang, Z. and Gursul, I., 2006, "Effect Of Spanwise Flexibility On Flapping Wing Propulsion," AIAA Paper 2006-2870, *36th AIAA Fluid Dynamics Conference and Exhibit*, (San Francisco, Ca, 5-8 June, 2006).

Isogai, K., Shinmoto, Y. and Watanabe, Y., 1999, Effects of Dynamic Stall on Propulsive Efficiency and Thrust of Flapping Airfoil, *AIAA Journal*, Vol. 37(10) pp. 1145~1151.

Jones, K. D., Dohring, C. M. and Platzer, M. F., 1996, "Wake Structures Behind Plunging Airfoils: A Comparison of Numerical and Experimental Results." AIAA Paper 96~0078, *in 34th Aerospace Sciences Meeting and Exhibit* (Reno, Nevada, 1996).

Koochesfahani, M. M., 1989, "Vortical Patterns in the Wake of an Oscillating Airfoil," *AIAA Journal*, Vol. 27( 9), pp. 1200~1205.

Lai, J. C. S. and Platzer, M. F., 1999, "Jet Characteristics of a Plunging Airfoil," *AIAA Journal*, Vol. 37(12), pp. 1529~1537.

Lighthill, M. J., 1960, "A Note on the Swimming of Slender Fish," *Journal of Fluid Mechanics*, Vol. 9, pp. 305~317.

Schouveiler, L., Hover, F. S. and Triantafyllou, M. S., 2005, "Performance Of Flapping Foil Propulsion," *J. Fluids and Structures,* Vol. 20, pp. 949~959.

Shyy, W., Berg, M. and Ljungqvist, D., 1999, "Flapping and Flexible Wings for Biological and Micro Air Vehicles," *in Progress in Aerospace Sciences*, Vol. 35, pp. 455~505.

Triantafyllou, G. S., Triantafyllou, M. S. and Grosenbaugh, M. A., 1993, "Optimal Thrust Development in Oscillating Foils with Application to Fish Propulsion," *Journal of Fluids and Structures*, Vol. 7, pp. 205~224.

Young, J. and Lai, J. C. S., 2004, "Oscillation Frequency and Amplitude Effects on the Wake of a Plunging Airfoil," *AIAA Journal*, Vol. 42(10), pp. 2042~2052.